11

Defect modes of photonic crystal with conducting nanolayer on insulating substrate

© A.V. Skripal, D.V. Ponomarev, V.E. Sharonov

Saratov National Research State University,
410012 Saratov, Russia
e-mail: skripala_v@info.sgu.ru

Received March 26, 2024
Revised October 23, 2024
Accepted November 1, 2024

The appearance of the defect mode in the band gap of the one-dimensional photonic crystal with dielectric filling, caused by the volumetric defect of the periodicity of the structure in the presence of conducting nanolayers deposited on insulating substrates, has been studied. Experimental data confirm the results of calculations of amplitude-frequency characteristics performed using the transfer matrix method and demonstrate the appearance of a defect mode in the bandgap in the X-band at certain values of the thickness $100-140$ nm and electrical conductivity of conducting nanolayers $7-200\,\Omega$/sq. The distribution of the electric field strength of an electromagnetic wave inside a photonic crystal with introduced conducting nanolayer into a defect has been calculated at the defect mode frequency for different ratios between the longitudinal size of the defect and the wavelength. Taking into account the field strength distribution in the defect layer of a photonic crystal makes it possible to provide both the transparency effect of a photonic crystal with a conducting nanolayer at the defect mode frequency and the effect of the defect mode suppression. The effects of nonreciprocal wave propagation in a photonic crystal associated with changes in the absorption coefficient have been described. It has been established that the degree of the nonreciprocity effect is determined by the level of interaction of the electromagnetic wave with the structure under study. The possibility of achieving high sensitivity to measure conducting structures based on the analysis of the defect mode of a photonic crystal has been noted.

Keywords: photonic crystal, conducting nanolayer, defect mode, nonreciprocity.

DOI: 10.61011/TP.2025.01.60519.102-24

Introduction

The unique properties of Bragg structures, often called photonic crystals (PC), are attributable to interference effects that occur when electromagnetic radiation interacts with them [1–4]. The occurrence of resonant effects in Bragg structures of the microwave and subterahertz ranges makes it possible to create various types of microwave devices based on them, for example, resonators with semiconductor detectors, directional couplers, miniature resonant antennas, matched loads, various types of microwave filters, including those with controlled characteristics, microwave sensors [5–12].

A number of resonant effects can be caused by both volumetric disturbances of the periodicity of the Bragg structure (the appearance of defective modes) and the peculiarities of its interface.

The ability to calculate the characteristics of defective modes of microwave Bragg structures with an accuracy that allows for a good match with the experiment is used for non-destructive testing of dielectrics, polar liquids, composites, structures with semiconductor layers [4,13].

The studied item (dielectric, semiconductor, polar liquid layer, etc.) in this case is inserted into the PC structure, most often into its central layer. A change of the frequency, amplitude, and quality of the defective mode is recorded depending on the properties of the item. However, when studying highly conductive semiconductor and metallic nanolayers and materials with high dielectric losses, limitations occur due to the almost complete disappearance of the defective mode in the band gap.

The occurrence of surface Tamm states in the PC of the optical and microwave ranges can be considered as interface states [14–20]. The authors of Ref. [18] theoretically substantiated and experimentally confirmed the possibility of Tamm resonances occurring at the edge of both the first and second forbidden bands of a one-dimensional microwave PC bordering a metal nanolayer or a nanolayer made in the form of parallel metal strips, at a certain range of thicknesses and electrical conductivity of the nanolayer. Since pronounced Tamm resonance was observed upon contact of PC with a metal nanolayer only at certain thicknesses and specific electrical conductivities of the nanolayer, in order to expand the ranges of electrical conductivity and thickness of the conductive layer at which pronounced Tamm resonances are observed, it was proposed in Ref. [21] to control the frequency of the Tamm resonance by changing the thickness the outermost layer of the photonic crystal bordering the conductive layer.

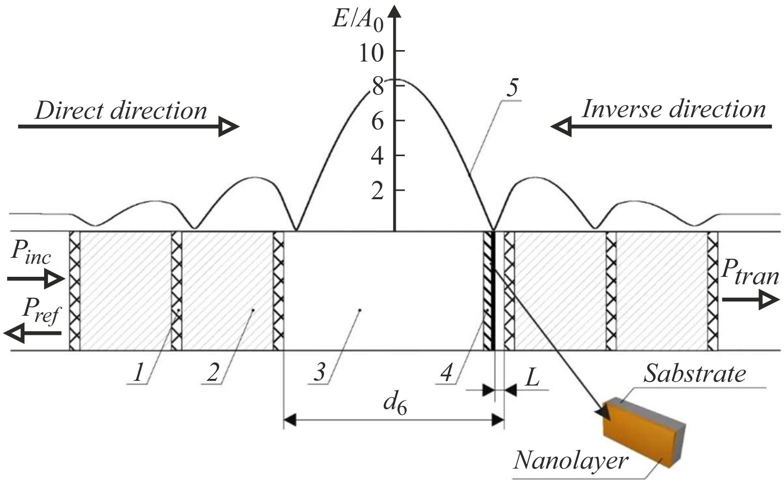

Figure 1. The distribution of the amplitude of the standing wave along the photonic crystal with a disturbance of $d_6 = 22$ mm and the longitudinal section of the photonic crystal: *1* — a layer of polycor, 1.0 mm thick, *2* — a layer of Teflon, 9.0 mm thick, *3* — disturbance, *4* — the structure under study is at a distance of L from the edge of the disturbance, *5* — the amplitude of the standing wave.

However, the electric field of the electromagnetic wave is concentrated in the PC layer bordering the conductive layer in case of implementation of the Tamm resonance, for this reason a change of the parameters of this PC layer is not sufficiently effective, although it leads to a change in the characteristics of the photonic Tamm resonance. At the same time, the location of the test sample in the area of concentration of the electromagnetic wave field can increase the efficiency of controlling resonant features on the frequency response of the PC. Since the area of concentration of the electric field is located inside the PC, when the sample is located in this area, a resonant feature is realized on the frequency response of the PC, which is usually called the defective mode [23–25].

The authors of [26] found that a small-sized conductive element in a disturbance leads to a slight decrease of the frequency of the defective mode, the magnitude of which depends on the location of this element and the size of the disturbance. The authors of Ref. [14] used the measured dielectric sample as a disturbance in the coaxial PC, implemented an frequency response with two forbidden bands, in each of which a defective mode appeared. The mode for which the defect appeared to be located in the antinode of the standing wave was used to measure the dielectric permittivity.

We consider in this paper the features of the amplitude-frequency characteristics of the reflection and transmission coefficients of a one-dimensional microwave waveguide photonic crystal in the presence of a defective mode caused by the creation of a periodicity disturbance, inside which a structure with a conductive nanolayer is located. Cases are considered when the size of the disturbance is significantly larger than the longitudinal size of the structure with a conductive nanolayer, and commensurate with it. The characteristics of the defective mode are analyzed when the electrical conductivity of the conductive layer changes over a wide range of values, based on taking into account the distribution of the electric field inside the disturbance of the PC, depending on the direction of propagation of the electromagnetic wave.

1. Simulation of a microwave photonic crystal with a disturbed layer

The microwave PC was a segment of a rectangular waveguide filled with two types of dielectric layers with different permittivity and thickness. The number of layers, equal to eleven, was selected from the sufficiency condition to obtain a pronounced band structure in the X-range of the amplitude-frequency characteristics of the photonic crystal. The disturbance was the central layer, made in the form of a segment of a waveguide with air filling.

The dielectric permittivity of the odd layers of the photonic crystal was chosen to be equal to $\varepsilon = 9.6$ (Al_2O_3) for simulation, thickness was -1.0 mm, even layers $\varepsilon = 2.0$ (Teflon), thickness 9.0 mm.

The studied structure, which is a nanometer-thick metal layer deposited on a ceramic substrate (Al_2O_3) with a thickness of 0.5 mm, was placed inside a disturbance of a photonic crystal, completely filling the cross section of the waveguide (Fig. 1).

2. Computer simulation of the characteristics of the defective mode of a microwave photonic crystal

To calculate the frequency dependences of the reflection coefficients $S_{11}(\omega)$ and the transmission coefficient $S_{21}(\omega)$ of an electromagnetic wave, a matrix of transmission of a layered structure with different values γ_i and γ_{i+1} of the propagation constants of electromagnetic waves for H_{10} type was used [4,6,27,28]:

$$T(z_{j,j+1}) = \begin{pmatrix} \frac{\gamma_{j+1}+\gamma_j}{2\gamma_{j+1}} \exp\Big((\gamma_{j+1}-\gamma_j)z_{j,j+1}\Big) & \frac{\gamma_{j+1}-\gamma_j}{2\gamma_{j+1}} \exp\Big((\gamma_(j+1)+\gamma_j)z_{j,j+1}\Big) \\ \frac{\gamma_{j+1}-\gamma_j}{2\gamma_{j+1}} \exp\Big(-(\gamma_{j+1}+\gamma_j)z_{j,j+1}\Big) & \frac{\gamma_{j+1}+\gamma_j}{2\gamma_{j+1}} \exp\Big(-(\gamma_{j+1}-\gamma_j)z_{j,j+1}\Big) \end{pmatrix}, \quad (1)$$

which relates the coefficients A_j, B_j and A_{j+1}, B_{j+1}, which determine the amplitudes of incident and reflected waves on both sides of the boundary $z_{j,j+1}$, by the ratio

$$\begin{pmatrix} A_{j+1} \\ B_{j+1} \end{pmatrix} = T(z_{j,j+1}) \cdot \begin{pmatrix} A_j \\ B_j \end{pmatrix}. \quad (2)$$

The coefficients of reflection S_{11} and transmission S_{21} of an electromagnetic wave interacting with a layered structure were determined through the elements of the transmission matrix T_N using the relations

$$S_{11} = -\frac{T_N[2,1]}{T_N[2,2]},$$

$$S_{21} = \frac{T_N[1,1]T_N[2,2] - T_N[1,2]T_N[2,1]}{T_N[2,2]}, \quad (3)$$

where

$$T_N = \begin{pmatrix} T_N[1,1] & T_N[1,2] \\ T_N[2,1] & T_N[2,2] \end{pmatrix} = \Pi^0_{j=N} T_{j,(j+1)}$$

$$= T(z_{N,N+1}) \cdot T(z_{N-1,N}) \ldots T(z_{1,2}) \cdot T(z_{0,1}) \quad (4)$$

the transmission matrix of a layered structure consisting of N layers. The propagation constants of the electromagnetic wave γ_0, γ_d, γ_m , respectively, in an empty waveguide, in dielectric layers, and in a conductive layer completely filling the waveguide in cross-section, were calculated using the expressions:

$$\gamma_0 = \sqrt{\frac{\pi^2}{a^2} - \omega^2\varepsilon_0\mu_0}, \quad (5)$$

$$\gamma_d = \sqrt{\frac{\pi^2}{a^2} - \omega^2\varepsilon_d\varepsilon_0\mu_0}, \quad (6)$$

$$\gamma_m = \sqrt{\frac{\pi^2}{a^2} - \omega^2\varepsilon^*_m\varepsilon_0\mu_0}, \quad (7)$$

where $\varepsilon^*_m = \varepsilon'_m - j\varepsilon''_m$ is the complex permittivity of the conductive layer; $\varepsilon'_m = \varepsilon_m - \frac{\sigma_m^2 m_m^*}{\varepsilon_0 e^2 n_m}$, $\varepsilon''_m = \frac{\sigma_m}{\varepsilon_0\omega}$; ε_m, σ_m, m^*_m, n_m — relative permittivity of the lattice, the specific electrical conductivity of the conductive layer, the effective mass and concentration of electrons in the conductive layer, respectively; a — the size of the wide wall of the waveguide; $\omega = 2\pi f$ – the circular frequency of the electromagnetic wave; ε_0 and σ_0 — electric and magnetic constants; ε_d — relative permittivity of the dielectric layer.

A wave equation of the form was used to describe the distribution of the electric field $E(z)$ in a one-dimensional photonic crystal:

$$\frac{\partial^2 E(z)}{\partial z^2} + \gamma^2(z)E(z) = 0, \quad (8)$$

where $\gamma(z)$ — electromagnetic wave propagation constant.

The solution of the wave equation inside each of the regions of a one-dimensional photonic crystal with an electromagnetic wave propagation constant γ_j can be represented as a superposition of incident and reflected waves and calculated using the following relation:

$$E_j = (T_j[1,1]A_0 + T_j[1,2]B_0) \cdot \exp(\gamma_j(z_{j+1} - z_j))$$
$$+ (T_j[2,1]A_0 + T_j[2,2]B_0) \cdot \exp(-\gamma_j(z_{j+1} - z_j)), \quad (9)$$

where $T_j[1,1]$, $T_j[1,2]$, $T_j[2,1]$, $T_j[2,2]$ are the elements of the transmission matrix of a layered structure consisting of j layers arranged sequentially.

The longitudinal dimensions of d_6 disturbances were 3.0 and 22.0 mm. In the first case, at the frequency of the defective mode, half the length of the electromagnetic wave $\lambda/2$ exceeds the electrical length of the disturbance $\varepsilon^{1/2}d_6$, and a standing wave node is observed in the center of the disturbance. In the second case, the size of the inhomogeneity along the direction of wave propagation is commensurate with half the wavelength λ at the frequency of the defective mode. The antinode of the standing wave is observed in the area of disturbance at the frequency of the defective mode [14,26]. In this case, the specific parameters of the photonic crystal and the disturbances were selected from the condition that a band gap was realized in a wide frequency band of the X band, and a defective mode occurred at a frequency close to the middle of the band gap.

The antinode of the standing wave was observed in the center of the disturbance with the size of the disturbance of $d_6 = 22$ mm, and nodes of the standing wave appeared near its boundaries inside the disturbance (Fig. 1).

It is possible to achieve a different level of interaction of the electromagnetic wave with it by moving the studied structure inside the disturbance.

Samples with a conducting layer thickness of $l = 20$ nm and a specific electrical conductivity of σ in the range from 10^0 to $10^7\,\Omega^{-1}\cdot\mathrm{m}^{-1}$ were considered. As follows from the calculation results, when the metal film is located in the node of the standing wave (at a distance of $L = 1.35$ mm from the boundary of the disturbance), the transmission coefficient S_{21} at the frequency of the defective mode with a change in the electrical conductivity of the sample from 10^0 to $10^7\,\Omega^{-1}\cdot\mathrm{m}^{-1}$ decreases from -0.01 to -4.5 dB. Such a slight decrease of the coefficient of passage S_{21} through a sample with high electrical conductivity can be interpreted as the realization of the effect of resonant tunneling through a conductive medium at frequencies lower than the frequency of plasma resonance [29].

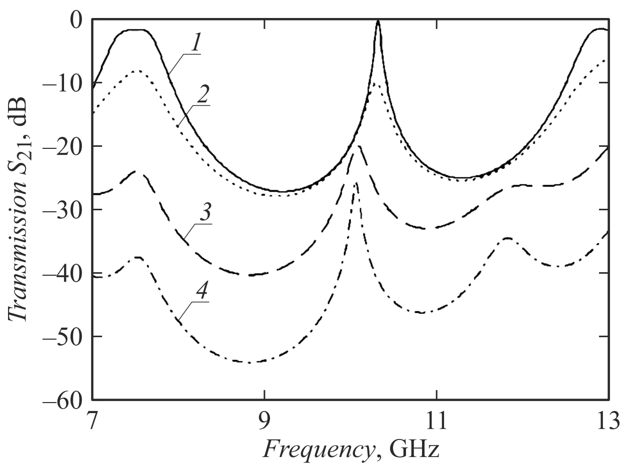

Figure 2. Frequency response of PC with a conductive nanolayer 20 nm thick at the boundary of the disturbance and different electrical conductivity of the nanolayer σ, $[\Omega^{-1} \cdot m^{-1}]$: *1* — without film, *2* — 10^5, *3* — $2 \cdot 10^6$, *4* — 10^7. The thickness of the nanolayer is 20 nm.

When the sample is located far from the node, for example, at the very edge of the disturbance ($L = 0.0$ mm), the transmission coefficient S_{21} at the frequency of the defective mode with a change in electrical conductivity σ of the sample is from 1 to $10^7\,\Omega^{-1} \cdot \mathrm{m}^{-1}$ decreases from -0.3 to -25 dB (fig. 2)

It should be noted that dielectric layers with a higher dielectric permittivity can be used in the structure of a photonic crystal, for example, layers of semi-insulating GaAs to increase the transmission coefficient of an electromagnetic wave at the frequency of the defective mode, when a sample with high electrical conductivity is located near the node of the standing wave.

As follows from the calculation results, an increase of the dielectric permittivity of odd layers from 9.6 (Al_2O_3) to 12.5 (GaAs) leads to an increase of the transmission coefficient in the presence of a conductive film with a conductivity of $10^7\,\Omega^{-1} \cdot \mathrm{m}^{-1}$ from -1.4 to -0.8 dB. This corresponds to a change of the transmission ratio from 72 to 83%.

The authors of Ref. [26] used small inclusions compared to the cross section of the waveguide to realize a pronounced defective mode in the frequency response of the PC when a conductive inclusion was introduced in disturbance. However, the sensitivity of the defective mode to the parameters of such an inclusion sharply decreases in this case.

The presented results make it possible to solve in many ways the problem of achieving high sensitivity in the characterization of conductive structures by introducing large-area conductive structures (completely filling the cross-section of the waveguide) into the disturbance. Since taking into account the field distribution in a photonic crystal makes it possible to choose the structure of the disturbed layer, which makes it possible to implement a pronounced defective mode even with the introduction of a large-area conductive structure.

The analysis of the obtained results also allows making a conclusion that a frequency shift of the defective mode can be observed with an increase of the electrical conductivity of the structure. In this case, the magnitude and sign of this displacement are determined by the location of the structure inside the disturbance. When the metal film is located inside, there is no disturbance in the node of the standing wave of the frequency shift of the defective mode. When the sample is located near the boundary of the disturbance, at a distance less than $L = 1.35$ mm, a frequency shift of the defective mode to the low frequency region is observed, and when located at a distance greater than 1.35 mm, a frequency shift of the defective mode to the high frequency region is observed. The greater the magnitude of the shift, the further the sample is located from the node of the electric field. It should be noted that since two nodes of the electric field are observed inside the disturbance near opposite boundaries of the disturbance, when the sample is moved from one node to the second at a distance at which the sample becomes closer to the second node than to the first, the magnitude of the frequency shift will decrease.

It should be noted that, depending on the direction of propagation of the wave through the photonic crystal, the value of the absorption coefficient of the electromagnetic wave in the nanolayer changes (Fig. 3), depending on the position of the sample inside the disturbance, especially with high conductivity of the nanolayer, which is associated with a change in its reflection coefficient, while the transmission coefficient remains unchanged.

When the metal nanolayer is located near the node of the standing wave, the resonant frequencies of the defective mode of reflection coefficients S_{11} and S_{22} for both directions of wave propagation in a photonic crystal coincide with the resonant frequency $f_0 = 10.132$ GHz of the defective mode of transmission coefficient S_{21}, the resonant frequency of which remains constant for both directions of wave propagation (Fig. 3, *a*). However, the Q-factor of the resonances S_{11} and S_{22} differs by more than 5 times. In this case, the Q-factor of the resonance of the reflection coefficient S_{11} (curve *3* in Fig. 3, *a*) in the forward direction of wave propagation coincides with the Q-factor of the resonance of the transmission coefficient S_{21} (curve *5* in Fig. 3, *a*).

When the metal nanolayer is located far from the node of the standing wave, for example, at the boundary of the disturbance $L = 0.0$ mm, the resonant frequency of the defective mode of the reflection coefficient (curve *2* in Fig. 3, *b*) for the reverse direction of wave propagation in the photonic crystal does not match the resonant frequency of the defective mode of the transmission ratio (curve *5* in Fig. 3, *b*).

The resonant frequency $f_1 = 9.84$ GHz of the defective mode S_{11} (curve *1* in Fig. 3, *b*), at which S_{11} is minimal, coincides with the resonant frequency of the defective

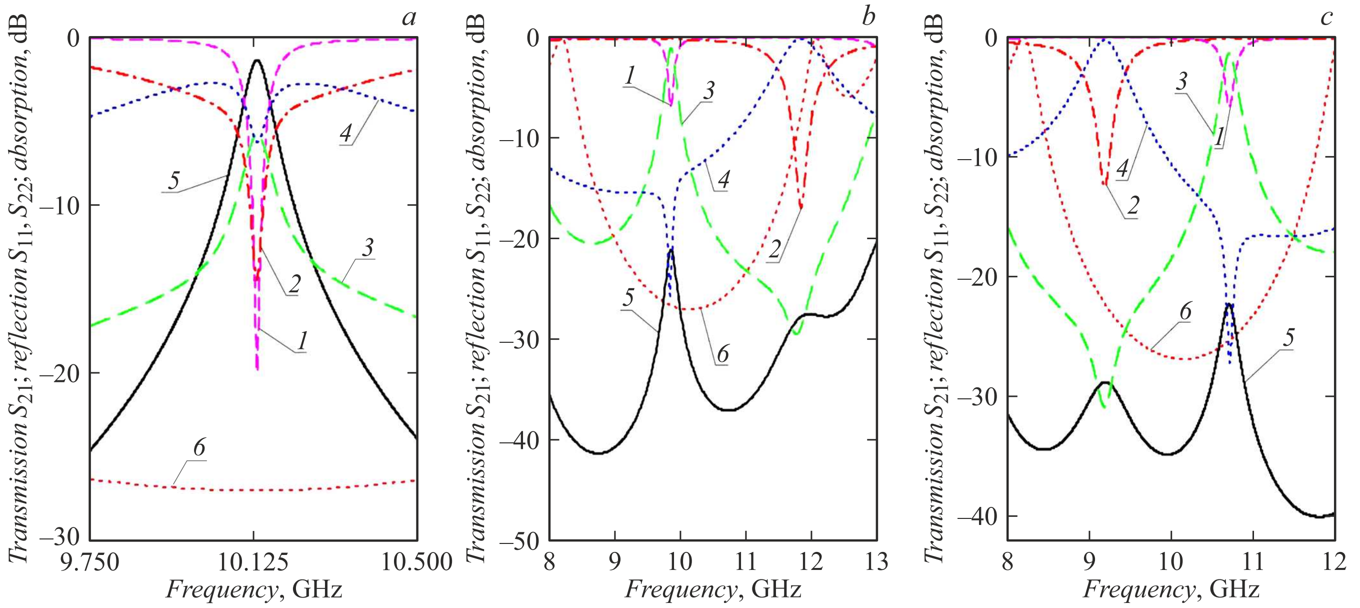

Figure 3. Calculated frequency response of reflection coefficients $S_{11}(f)$ (curves *1*) and $S_{22}(f)$ (curves *2*), absorption (curves *3, 4*) and transmission $S_{21}(f)$ (curves *5*) PC at different positions of the sample inside the disturbance, L, mm: a — 1.35, b — 0.0, c — 2.5, for two opposite directions of wave propagation (curves *1, 3* — straight direction, curves *2, 4* — reverse direction), frequency response of the photonic crystal transmission coefficient without violating the periodicity (curve *6*). $\sigma = 2.5 \cdot 10^6\,\Omega^{-1} \cdot \mathrm{m}^{-1}$, $l = 20$ nm, $d_6 = 22$ mm.

modes S_{21} (curve *5* in Fig. 3, *b*), and the absorption coefficient at this frequency is maximal (curve *3* in Fig. 3, *b*).

On the contrary, S_{22} reaches a value of -0.05 dB at a frequency of 9.84 GHz, and the absorption coefficient is minimal. This ensures that the transmission coefficient remains at the same level regardless of the direction of wave propagation.

The frequency dependence of the reflection coefficient S_{22} is characterized by resonance at a frequency of $f_2 = 11.83$ GHz ($S_{22} = -16.9$ dB). At this frequency, a weakly pronounced local maximum of S_{21} at the level of -27.5 dB is due to the maximum absorption coefficient, and S_{22} is minimal and weakly affects S_{21}.

Fig. 3, *c* shows the frequency response of the PC when the sample is located at a distance of $L = 2.5$ mm, at which a frequency shift of the maximum transmission coefficient of the defective mode to the high frequency range of $f_3 = 10.7$ GHz is observed.

Considering the effect of the dependence of the absorption coefficient of an electromagnetic wave in a conductive nanolayer on the direction of wave propagation through a photonic crystal, it can be concluded that the degree of manifestation of the effect is determined by the level of interaction of the electromagnetic wave with the structure under study, which depends on the electric field strength at the location of the nanolayer.

Since changing the parameters of the periodicity disturbance leads to a change in the frequency of the defective mode, reducing the size of the disturbance to $d_6 = 3$ mm allows the defective mode to be realized at a frequency close to the middle of the band gap, as well as at $d_6 = 22$ mm.

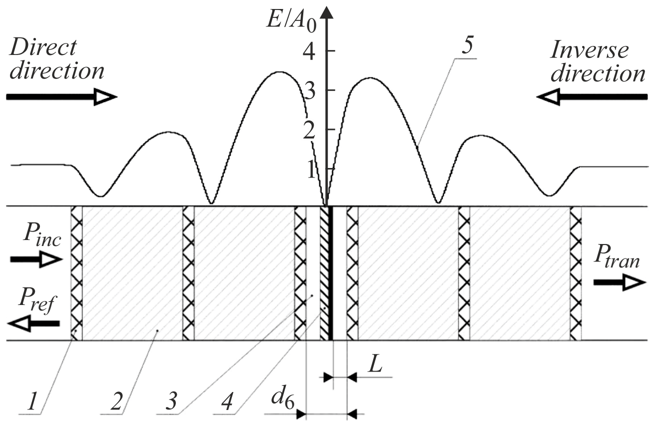

Figure 4. The distribution of the amplitude of the standing wave along the photonic crystal with a disturbance of $d_6 = 3$ mm and the longitudinal section of the photonic crystal: *1* — a layer of polycor, 1.0 mm thick, *2* — a layer of Teflon, 9.0mm thick mm, *3* — disturbance, *4* — the structure under study is at a distance of L from the edge of the disturbance, *5* — the amplitude of the standing wave.

However, in this case, a standing wave node is observed in the center of the disturbance (Fig. 4).

The results of calculating the frequency response of PC with a disturbance of $d_6 = 3$ mm, shown in Fig. 5, for the case of the location of a conductive nanolayer in the middle of the disturbance indicate the realization of the transparency effect of a photonic crystal with a conductive nanolayer, in which the resonant frequency of the defective

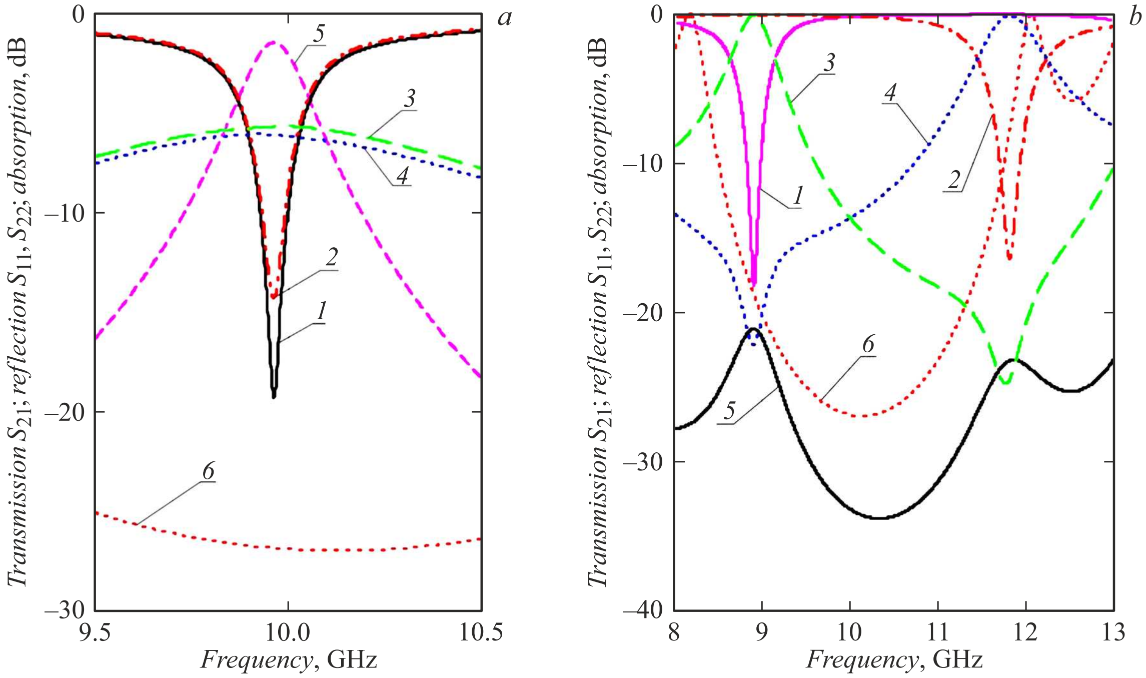

Figure 5. Calculated frequency response $S_{11}(f)$ (curves *1*), $S_{22}(f)$ (curves *2*), absorption (curves *3, 4*) and passage $S_{21}(f)$ (curves 5), PC at different positions of the sample inside the disturbance, L, mm: a — 1.5, b — 0.0, for two directions of wave propagation (curves *1, 3* — straight lines, curves *2, 4* — the opposite), frequency response $S_{21}(f)$ PC without disturbance of periodicity (curve *6*). $\sigma = 2.5 \cdot 10^6\,\Omega^{-1} \cdot \text{m}^{-1}$, $l = 20$ nm, $d_6 = 3.0$ mm.

mode of the reflection coefficient for both directions of wave propagation in the photonic crystal coincides with the resonant frequency of the defective transmission coefficient mode (Fig. 5, *a*), which remained unchanged compared to the frequency of the defective mode in the case of the absence of a conductive nanolayer. When the conductive nanolayer is located at the boundary of the disturbance, the effect of the dependence of the absorption coefficient of an electromagnetic wave in the conductive nanolayer on the direction of wave propagation through the photonic crystal is manifested (Fig. 5, *b*).

3. Experimental study of the resonance characteristics of microwave photonic crystals

A one-dimensional photonic crystal created in accordance with the model described above was experimentally studied in the frequency range of 7−13 GHz.

The experimental model of the PC is made from a set of alternating plane-parallel plates, which were placed in a section of the waveguide with a section 23×10 mm. The dielectric permittivity ε of the plates forming eleven odd and even photonic crystal layers with a thickness of 1.0 and 9.0 mm was measured using the AgilentPNA-X Network Analyzer N5242A vector circuit analyzer and determined using Agilent 85071E Materials Measurement Software [30] and amounted to $\varepsilon = 9.6$ (Al_2O_3) and 2.0 (Teflon), respectively. A periodicity disturbance was created in the photonic crystal in the form of replacing the central layer of Teflon with an air segment 22 mm long.

The studied samples in the form of a plate (Al_2O_3) 0.5 mm thick with a TaAlN resistive layer were inserted into the disturbed PC layer. The TaAlN layer was applied by thermal evaporation in a vacuum. The studied samples were characterized by the surface resistance ρ_l in the range of 7−200 Ω/sq and thicknesses of $l = 100 - 140$ nm.

The thickness of the conductive nanolayer was measured using the „step" method with Agilent 5600 atomic force microscope. The specific surface resistance was measured using a four-probe method using the Jandel RMS-EL-Z probe station.

The frequency dependences $S_{11}(f)$, $S_{22}(f)$, $S_{21}(f)$ of a photonic crystal at different positions of structures with a nanolayer with different surface resistance and thickness inside the disturbance were studied using the AgilentPNA-X Network Analyzer N5242A vector circuit analyzer.

In accordance with the results of the theoretical analysis, it was experimentally possible to observe changes in the frequency and amplitude of the defective PC mode with a decrease of ρ_l nanolayer when placed at the boundary of the PC disturbance (Fig. 6). The frequency shift of the defective mode was about −200 MHz with a change in the surface resistance of ρ_l nanolayer from 200 to 7 Ω/sq.

It has also been experimentally determined that when a conductive film with a surface resistance of ρ_l is located

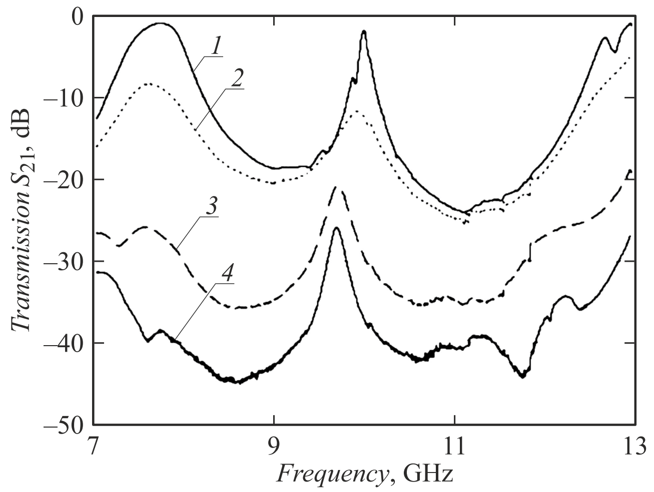

Figure 6. Experimental frequency response of PC with a conductive nanolayer at the boundary of the disturbance and various surface resistances of the nanolayer ρ_l, Ω/sq: *1* — without film, *2* — 210, *3* — 20.0, *4* — 7.0. $d_6 = 22$ mm.

in the range of values of $7-200\,\Omega$/sq at a distance of ~ 1.6 mm from the boundary of the disturbance corresponding to the node for a standing wave, the decrease in the transmission coefficient S_{21} did not exceed -5.0 dB, and the frequency shift of the defective mode was not observed. When the conductive film ($\rho_l = 7\,\Omega$/sq) was positioned at a distance of ~ 3.0 mm, a frequency shift was observed and amounted to about 400 MHz.

Experimentally, several types of resonances on the frequency response of the reflection coefficient in the band gap PC were observed, depending on the location of the nanolayer inside the disturbance, the magnitude of the nanolayer's conductivity, and the direction of propagation of the electromagnetic wave (Fig. 7).

When the conductive nanolayer is located near the node of the standing wave at all values of its surface resistance in the range from 200 to 7 Ω/sq, the resonant frequencies of the defective mode of the reflection coefficient for the straight line (curve *1* in Fig. 7, *a*) and the reverse (curve *2* in Fig. 7, *a*) directions of wave propagation in a photonic crystal coincide with the resonant frequency of the defective mode of the transmission coefficient (curve *3* in Fig. 7, *a*). At the same time, as follows from the results of computer modeling, resonances are characterized by different Q-factor values (curves *1* and *2* in Fig. 7, *a*).

When a structure with a conductive nanolayer with low surface resistance (high surface conductivity) is located inside the disturbance both to the left and to the right of the standing wave node, the resonant frequency of the defective mode of the reflection coefficient is $S_{11}(f)$ (curves *1* in Fig. 7, *b* and *c*) coincides with the resonant frequency of the defective mode $S_{21}(f)$ (curves *3* in Fig. 7, *b* and *c*), and the resonant frequency of the defective mode of the reflection coefficient $S_{22}(f)$ (curves *2* in Fig. 7, *b* and *c*) does not match the resonant frequency of the defective mode $S_{21}(f)$. The resonant frequency of the defective mode $S_{22}(f)$ is greater than the resonant frequency of the defective mode $S_{21}(f)$ at $L = 0.0$ mm, and the resonant frequency of the defective mode $S_{22}(f)$ at $L = 2.5$ mm is less than the resonant frequency of the defective mode $S_{21}(f)$. This behavior of the frequency response confirms the results of computer modeling performed by the transfer matrix method.

Conclusion

The frequency response of the reflection and transmission coefficients of a one-dimensional microwave waveguide photonic crystal in the presence of a defective mode caused by the creation of a periodicity disturbance, inside which a metal dielectric structure with a conductive nanolayer is located.

The characteristics of the defective mode are analyzed when the electrical conductivity of a conductive nanolayer changes over a wide range of values, based on taking into account the distribution of the electric field inside a disrupted photonic crystal depending on its size.

It is shown that, depending on the ratio between the longitudinal size of the disturbance and the standing wavelength inside a photonic crystal, both the transparency effect of a photonic crystal with a conductive nanolayer at the frequency of the defective mode and the suppression effect of the defective mode are realized with different structures of the disturbed layer.

It was found that the frequency position of the defective mode of the transmission coefficient at a fixed position of the sample inside the disturbance changes with a decrease in the surface resistance of the conductive nanolayer. In this case, the magnitude and sign of this change are determined by the location of the structure inside the disturbance.

It is shown that, depending on the direction of wave propagation through a photonic crystal, the absorption of an electromagnetic wave in a conductive nanolayer changes, determined by the level of interaction of the electromagnetic wave with the structure under study, which depends on the electric field strength at the location of the nanolayer.

The results obtained can be used to achieve high sensitivity to thickness and specific electrical conductivity when characterizing highly alloyed semiconductor and metallic nanolayers, graphene structures, and metal-dielectric metasurfaces by introducing large-area conductive structures into the breach.

Funding

This study was supported by grant № 25-22-00199 from the Russian Science Foundation.

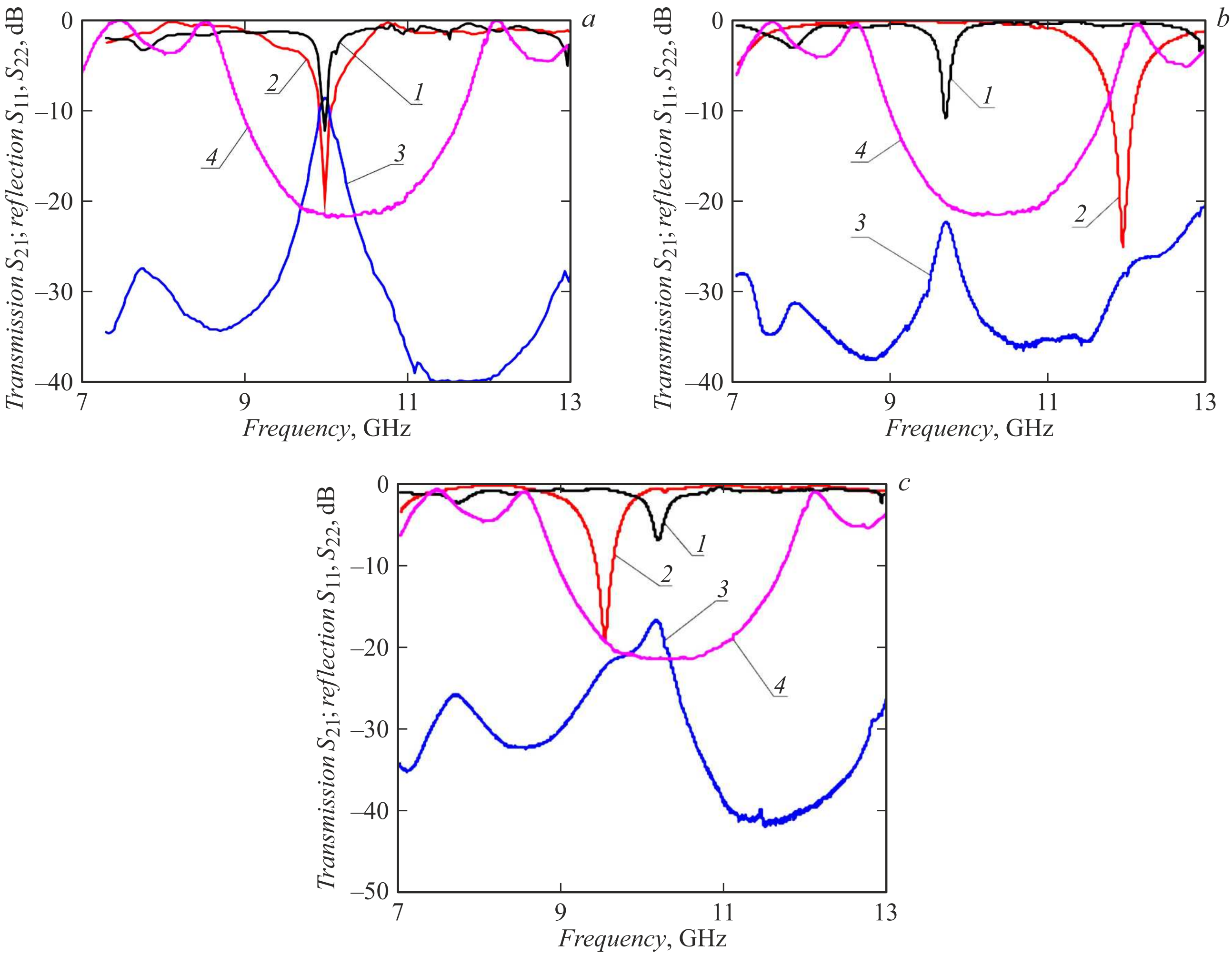

Figure 7. Experimental frequency response $S_{11}(f)$ (curves *1*), $S_{22}(f)$ (curves *2*), and $S_{21}(f)$ (curves *3*) PC at various positions the sample inside the disturbance, L, mm: a — 1.6, b — 0.0, c — 2.5. Frequency response $S_{21}(f)$ of a photonic crystal without periodicity disturbance (curve *4*). $l = 140$ nm, $\rho_l = 19.5\,\Omega$/sq, $d_6 = 22$ mm.

Conflict of interest

The authors declare that they have no conflict of interest.

References

[1] M.V. Rybin, M.F. Limonov. Phys. Usp., **62** (8), 823 (2019). DOI: 10.3367/UFNe.2019.03.038543
[2] V.A. Tolmachev. Opt. Spectrosc., **122** (4), 646 (2017). DOI: 10.1134/S0030400X17030201
[3] C. Sibilia, T.M. Benson, M. Marciniak, T. Szoplik. *Photonic crystals: physics and technology* (Springer, Milan, 2008), DOI: 10.1007/978-88-470-0844-1
[4] D.A. Usanov, S.A. Nikitov, A.V. Skripal, D.V. Ponomarev. *One-dimensional microwave photonic crystals: new applications*. (CRC Press, Taylor Francis Group, Boca Raton, FL, USA, 2019), DOI: 10.1201/9780429276231
[5] V.M. Mukhortov, S.I. Masychev, A.A. Mamatov. Tech. Phys. Lett., **39** (10), 921 (2013). DOI: 10.1134/S1063785013100234
[6] A.A. Nikitin, A.A. Nikitin, A.B. Ustinov, B.A. Kalinikos, E. Lähderanta. Tech. Phys., **61** (6), 913 (2016). DOI: 10.1134/S106378421606013X
[7] B.A. Belyaev, S.A. Khodenkov, V.F. Shabanov. Dokl. Phys., **61** (4), 155 (2016). DOI: 10.1134/S1028335816040017
[8] B.A. Belyaev, V.F. Shabanov, S.A. Khodenkov, R.G. Galeev. Dokl. Phys., **64** (3), 85 (2019). DOI: 10.1134/S1028335819030017
[9] H.C.C. Fernandes, J.L.G. Medeiros, I.M.A. Junior, D.B. Brito. PIERS Online, **3** (5), 689 (2007). DOI: 10.2529/PIERS060901105337
[10] H.B. El-Shaarawy, F. Coccetti, R. Plana, M. El-Said, E.A. Hashish. WSEAS Trans. Comm., **7** (11), 1112 (2008).
[11] J. Yao, C. Yuan, H. Li, J. Wu, Y. Wang, A.A. Kudryavtsev, V.I. Demidov, Z. Zhou. AIP Advances, **9** (6), 065302(2019). DOI: 10.1063/1.5097194
[12] Tao Wei, Songping Wu, Jie Huang, Hai Xiao, Jun Fan. Appl. Phys. Lett., **99** (11), 113517 (2011). DOI: 10.1063/1.3636406
[13] Jie Huang, Tao Wei, Xinwei Lan, Jun Fan, and Hai Xiao. *Proc. SPIE 8345, Sensors and Smart Structures*

Technologies for Civil, Mechanical, and Aerospace Systems (San Diego, United States, 2012), 83452Z. DOI: 10.1117/12.915035
[14] D.A. Usanov, A.V. Skripal', D.V. Ponomarev, O.M. Ruzanov, I.O. Timofeev, S.A. Nikitov. J. Comm. Technol. Electron., **65** (5), 541 (2020). DOI: 10.1134/S1064226920040087
[15] R.G. Bikbaev, S.Ya. Vetrov, I.V. Timofeev. J. Opt., **19** (1), 015104 (2017). DOI: 10.1088/2040-8986/19/1/015104
[16] A.P. Vinogradov, A.V. Dorofeenko, A.M. Merzlikin, A.A. Lisyansky. Phys. Usp., **53** (3), 243 (2010). DOI: 10.3367/UFNe.0180.201003b.0249
[17] A.P. Vinogradov, A.V. Dorofeenko, S.G. Erokhin, M. Inoue, A.A. Lisyansky. Phys. Rev. B, **74** (4), 045128 (2006). DOI: 10.1103/PhysRevB.74.045128
[18] A.V. Skripal, D.V. Ponomarev, A.A. Komarov. IEEE Trans. Microw. Theory Tech., **68** (12), 5115 (2020). DOI: 10.1109/TMTT.2020.3021412
[19] D.P. Belozorov, A.A. Girich, S.V. Nedukh, A.N. Moskaltsova, S.I. Tarapov. PIER Lett., **46**, 7 (2014). DOI: 10.2528/PIERL13122502
[20] T. Goto, A.V. Dorofeenko, A.M. Merzlikin, A.V. Baryshev, A.P. Vinogradov, M. Inoue, A.A. Lisyansky, A.B. Granovsky. Phys. Rev. Lett., **101** (11), 113902 (2008). DOI: 10.1103/PhysRevLett.101.113902
[21] Al.V. Skripal, D.V. Ponomarev, A.A. Komarov, V.E. Sharonov. Izv. Sarat. Univ. Phys., **22** (2), 123 (2022). DOI: 10.18500/1817-3020-2022-22-2-123-130
[22] E. Yablonovitch, T.J. Gimitter, R.D. Meade. Phys. Rev. Lett., **67** (24), 3380 (1991). DOI: 10.1103/PhysRevLett.67.3380
[23] B.A. Belyaev, A.S. Voloshin, V.F. Shabanov. Dokl. Phys., **50** (7), 337 (2005). DOI: 10.1134/1.2005355
[24] V.A. Gunyakov, S.A. Myslivets, A.M. Parshin, V.Y. Zyryanov, V.G. Arkhipkin, V.F. Shabanov. Tech. Phys., **55** (10), 1484 (2010). DOI: 10.1134/S1063784210100142
[25] M. Inoue, A. Baryshev, H. Takagi, P.B. Lim, K. Hatafuku, J. Noda, K. Togo. Phys. Lett., **98**, 132511 (2011). DOI: 10.1063/1.3567940
[26] D.A. Usanov, A.V. Skripal', A.A. Romanov. Tech. Phys., **62** (6), 899 (2017). DOI: 10.1134/S1063784217060263
[27] S. Fan, M.F. Yanik, Z. Wang, S. Sandhu, M.L. Povinelli, J. Light. Technol., **24** (12), 4493 (2006). DOI: 10.1109/JLT.2006.886061.
[28] V.S. Gorelik, V.V. Kapaev. JETP, **123** (3), 373 (2016). DOI: 10.1134/S1063776116070062
[29] Al.V. Skripal, D.V. Ponomarev, V.E. Sharonov. Tech. Phys. Lett., **49** (10), 23 (2023). DOI: 10.21883/0000000000
[30] Electronic media. Available at: https://www.cmc.ca/wp-content/uploads/2019/08/Basics_Of_MeasuringDielectrics_5989-2589EN.pdf

Translated by A.Akhtayamov